

On Generating Explanations for Reinforcement Learning Policies: An Empirical Study

Mikihisa Yuasa¹, Huy T. Tran¹, and Ramavarapu S. Sreenivas²

Abstract—Understanding a *reinforcement learning* policy, which guides state-to-action mappings to maximize rewards, necessitates an accompanying explanation for human comprehension. In this paper, we introduce a set of *linear temporal logic* formulae designed to provide explanations for policies, and an algorithm for searching through those formulae for the one that best explains a given policy. Our focus is on explanations that elucidate both the ultimate objectives accomplished by the policy and the prerequisite conditions it upholds throughout its execution. The effectiveness of our proposed approach is illustrated through a simulated game of capture-the-flag and a car-parking environment.

I. INTRODUCTION

Reinforcement learning (RL) has revolutionized numerous domains due to its ability to autonomously acquire knowledge and make decisions in complex environments. The integration of deep learning techniques in RL, or *deep reinforcement learning* (DRL), has significantly advanced the field. DRL has allowed agents to surpass human experts in games like Chess and Go [1], enhance recommendation systems [2], and contribute to robotics [3]. However, the complexity of DRL models raises a significant concern: their lack of explainability or interpretability [4], [5]. As these systems advance to solve real-world problems, their decision-making processes grow more opaque, making it difficult to understand the reasoning behind their choices.

A common approach to explaining complex policies, such as those produced by DRL, is to mine *temporal logic* (TL) explanations from observed system behaviors and environment interactions [6]. TL offers a formal structure and interpretable semantics for describing the evolution of system states over time. Traditionally, methods are based on a classification problem setup, where positive (from the target policy) and negative (from another policy) trajectories are provided, with various techniques employed to optimize the classifier. For example, [7], [8] use directed acyclic graphs to simultaneously learn a *signal temporal logic* (STL) formula structure and its associated parameters. Tree-based algorithms [9], [10] have also been proposed to solve the same problem. More recently, neural networks have been used to learn parameters of a given *weighted signal temporal logic* (wSTL) formula structure [11]. Reference [12] extends [11] to learn STL formula structures. However,

all of these methods focus on identifying the formula that best differentiates the given positive and negative data; the inferred formula therefore strongly depends on how the given data were generated. Methods have also been developed that only require positive data, eliminating the need to generate negative data. References [13], [14] introduce a tightness metric that allows one to perturb positive data and estimate parameters of a given STL formula structure based on the resulting impact on tightness. Nonetheless, these methods remain biased by the given positive data.

In this work, we take a different approach where we assume access to the target policy itself, rather than being given a fixed set of positive and/or negative trajectories. The target policy could be accessible, for example, if one was optimizing a DRL policy for a complex task and wanted to gain insight into the underlying decision logic behind the policy to increase trust or support its verification in safety-critical applications. We are motivated by the idea that having access to the target policy will provide additional information that could help with the inference process. More specifically, we propose to use action distributions from the target policy to gain further insight into an agent’s preferences across possible actions for sampled states. This insight could be useful, for example, when an agent does not have a strong preference for the action taken in a given state (rather than strongly preferring one action); this lack of preference could help differentiate between possible explanations for that policy. Inferring such preferences from a fixed dataset (i.e., without access to the policy itself) is challenging, particularly for stochastic policies and environments. These preferences could also be used to emphasize informative states during the inference process, which may not have been visited in a given set of trajectories.

Based on this idea, we propose a greedy search method that infers the *linear temporal logic* (LTL) formula that best explains a target policy, where this explanation delineates both the operational conditions maintained throughout execution, as well as the ultimate objectives achieved by the policy. Our approach centers on a class of LTL formulae that is endowed with a concept of neighborhood (Sections III-A and III-C), which in turn is amenable to a local-search algorithm. In our method, each potential LTL-explanation is effectively translated into an RL policy using established techniques [15]. We then gauge the alignment of this representative policy with the target policy by employing a well-structured metric (Section III-B). Should a neighboring LTL-explanation exhibit superior alignment with the target policy according to this metric, it supplants the current explanation.

¹Aerospace Engineering, University of Illinois at Urbana-Champaign, Urbana, IL 61801 USA. {myuasa2, huytran1}@illinois.edu

²Industrial and Enterprise Systems Engineering, University of Illinois at Urbana-Champaign, Urbana, IL 61801 USA. rsree@illinois.edu

*This work was supported in part by ONR grant N00014-20-1-2249 and JASSO Study Abroad Support Program (Graduate Degree Program).

This iterative process persists until none of the neighboring LTL-explanations surpasses the present one, thus establishing a local optimum as the recommended LTL-explanation. To enhance robustness, we propose additional neighborhood expansion and extension heuristics (Section III-D), as well as a multi-start implementation of the search that generates the top- k (e.g., $k = 10$) LTL-explanations as candidate explanations. We demonstrate our method in two simulated environments: a game of capture-the-flag and a car-parking environment (Section IV).

II. BACKGROUND

A. Reinforcement Learning

We model our problem as a *Markov decision process* (MDP) \mathcal{M} defined by a tuple $(\mathcal{S}, \mathcal{A}, p, r, \gamma)$ [16], where \mathcal{S} is the state space, \mathcal{A} is the action space of the agent, and $\gamma \in [0, 1]$ is the discount factor. Then $p(s'|s, a) : \mathcal{S} \times \mathcal{A} \times \mathcal{S} \mapsto [0, 1]$ is the state transition function and $r(s, a, s') : \mathcal{S} \times \mathcal{A} \times \mathcal{S} \mapsto \mathbb{R}$ is the reward function for states $s, s' \in \mathcal{S}$ and action $a \in \mathcal{A}$. At time step t , the agent executes an action a_t given the current state s_t , after which the system transitions to state s_{t+1} and the agent receives reward $r(s_t, a_t, s_{t+1})$. Let $\pi(a|s) : \mathcal{S} \times \mathcal{A} \mapsto [0, 1]$ be a policy for the agent. The objective in RL is to learn a policy that maximizes the expected sum of discounted rewards $\mathbb{E}_{p, \pi} \{ \sum_{t=0}^{\infty} \gamma^t r(s_t, a_t, s_{t+1}) \mid s_0 = s, a_0 = a \}$ [17].

B. Linear Temporal Logic

Using Backus-Naur form, the syntax for LTL is defined as $\phi := \top \mid \psi(s) \mid \neg\phi \mid \phi \vee \phi' \mid \phi \wedge \phi' \mid \mathcal{G}(\phi) \mid \mathcal{F}(\phi) \mid \mathcal{U}(\phi) \mid \mathcal{X}(\phi)$ for logical formulae ϕ and ϕ' . Here, \top is the True Boolean constant, $s \in \mathcal{S}$ is an MDP state, $\psi(s) := f(s) < c$ is an atomic predicate over s for $c \in \mathbb{R}$, and \neg (negation), \wedge (conjunction), and \vee (disjunction) are Boolean connectives. \mathcal{F} (eventually), \mathcal{G} (globally), \mathcal{U} (until), and \mathcal{X} (next) are temporal operators. When presented with an LTL formula and a state or trajectory, we can assign a real-number value, the robustness, that reflects the degree to which the LTL formula is satisfied. In this context, a higher robustness value signifies a more substantial level of satisfaction. More formally, given a state $s \in \mathcal{S}$ and LTL formulae ϕ, ϕ' , the robustness of boolean operators is defined as,

$$\begin{aligned} \rho(s, f(s) < c) &= c - f(s), \\ \rho(s, \neg\phi) &= -\rho(s, \phi), \\ \rho(s, \phi \wedge \phi') &= \min(\rho(s, \phi), \rho(s, \phi')), \\ \rho(s, \phi \vee \phi') &= \max(\rho(s, \phi), \rho(s, \phi')). \end{aligned}$$

Given a trajectory of states $\tau := (s_0, s_1, \dots, s_k)$ and LTL formula ϕ , the robustness of temporal operators is defined as,

$$\begin{aligned} \rho(\tau, \mathcal{F}(\phi)) &= \max_{i \in [0, k]} (\rho(s_i, \phi)), \\ \rho(\tau, \mathcal{G}(\phi)) &= \min_{i \in [0, k]} (\rho(s_i, \phi)). \end{aligned}$$

C. FSPA-Augmented MDP

A feasible LTL formula can be transformed into a *Finite State Predicate Automaton* (FSPA) using ω -automaton manipulation with the help of model checking packages such as Spot [15], [18], [19]. More formally, an FSPA \mathcal{A} is defined by a tuple $(\mathcal{Q}, \mathcal{S}, \mathcal{E}, \Phi, q_0, b, F, Tr)$. Here, \mathcal{Q} is a finite set of automaton states, \mathcal{S} is an MDP state space, $\mathcal{E} \subseteq \mathcal{Q} \times \mathcal{Q}$ is the set of edges (transitions) between automaton states, Φ is the input alphabet, $q_0 \in \mathcal{Q}$ is the initial automaton state, $b : \mathcal{E} \mapsto \Phi$ maps an edge (q_t, q_{t+1}) to its transition condition (defined as an LTL formula ϕ), $F \subseteq \mathcal{Q}$ is the set of final (accepting) automaton states, and $Tr \subseteq \mathcal{Q}$ is the set of automaton trap states.

We now define an FSPA-augmented MDP $\mathcal{M}_{\mathcal{A}}$ based on the formulation in [15]. Given MDP \mathcal{M} and FSPA \mathcal{A} , an FSPA-augmented MDP $\mathcal{M}_{\mathcal{A}}$ is defined by a tuple $(\tilde{\mathcal{S}}, \mathcal{Q}, \tilde{\mathcal{A}}, \tilde{p}, \tilde{r}, \mathcal{E}, \Psi, q_0, b, F, Tr)$. Here, $\tilde{\mathcal{S}} \subseteq \mathcal{S} \times \mathcal{Q}$ is the product state space. Then $\tilde{p}(\tilde{s}'|\tilde{s}, a) : \tilde{\mathcal{S}} \times \mathcal{A} \times \tilde{\mathcal{S}} \mapsto [0, 1]$ is the state transition function and $\tilde{r}(\tilde{s}, a, \tilde{s}') : \tilde{\mathcal{S}} \times \mathcal{A} \times \tilde{\mathcal{S}} \mapsto \mathbb{R}$ is the reward function for states $\tilde{s}, \tilde{s}' \in \tilde{\mathcal{S}}$ and action $a \in \mathcal{A}$. We consider two rewards in this paper. For sparse reward settings, we define the reward \tilde{r} as,

$$\tilde{r}(\tilde{s}, a, \tilde{s}') = \begin{cases} 0 & q = q', \\ -\rho(s, b(q, q')) & q' \in Tr, \\ \rho(s, b(q, q')) & \text{otherwise,} \end{cases} \quad (1)$$

where $q, q' \in \mathcal{Q}$. For dense reward settings, we define the reward \tilde{r} as,

$$\tilde{r}(\tilde{s}, a, \tilde{s}') = \begin{cases} \beta \rho(s, b(q, q^*)) & q = q', \\ -\rho(s, b(q, q')) & q' \in Tr, \\ \rho(s, b(q, q')) & \text{otherwise,} \end{cases} \quad (2)$$

where $\beta \in [0, 1]$ is a scaling factor, $q^* = \arg \max_{q'' \in \mathcal{N}} \rho(s, b(q, q''))$, and $\mathcal{N} = \{q'' \in \mathcal{Q} \setminus Tr \mid (q, q'') \in \mathcal{E}\}$ is the set of non-trap automaton states that neighbors q . The intuition of this dense reward is that if the next automaton state is the same as the current automaton state, the reward encourages a transition to a non-trap automaton state.

III. METHOD

Our problem statement is as follows: given a target policy π_{tar} , MDP \mathcal{M} , and a set of atomic predicates Ψ , find an explanation ϕ that explains the objectives of the policy and the operational conditions maintained throughout execution. We address this problem by proposing a greedy local-search method, summarized in Figure 1 and Algorithms 1 and 2. We detail the key components of our method below.

A. Definition of LTL-Explanations

We consider the class of LTL-explanations of the form $\phi = \mathcal{F}(\phi_F) \wedge \mathcal{G}(\phi_G)$, where ϕ_F and ϕ_G are *Conjunctive Normal Form* (CNF) or *Disjunctive Normal Form* (DNF) formulae that have up to two clauses within them. We choose this form based on the assumption that the policy tries to achieve a task represented ϕ_F while satisfying global constraints

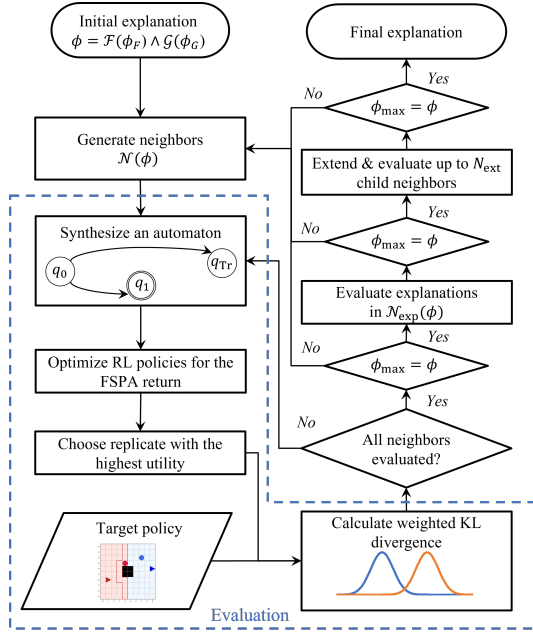


Fig. 1: Overview of our proposed search algorithm.

represented by ϕ_G . For example, given a set of atomic predicates $\Psi := \{\psi_0, \psi_1, \psi_2, \psi_3, \psi_4\}$, a possible explanation is $\mathcal{F}(\psi_0 \vee \psi_1) \wedge \mathcal{G}(\neg\psi_2 \wedge (\neg\psi_3 \vee \psi_4))$, which requires that: “Eventually, either ψ_0 or ψ_1 is satisfied. Globally, ψ_2 is not satisfied and either ψ_3 is not satisfied or ψ_4 is satisfied.”

We represent each LTL-explanation as a row vector of truth values whose length is $3N_{\text{pred}} + 2$, where $N_{\text{pred}} = |\Psi|$. The first N_{pred} elements of the vector define whether or not each predicate is negated (0 for no negation, 1 for negation). The next N_{pred} elements define which temporal formula, ϕ_F or ϕ_G , each predicate belongs to (0 for ϕ_F , 1 for ϕ_G). We require each temporal formula to contain at least one predicate. The following N_{pred} elements define which clause within the temporal formula each predicate belongs to (0 for the first clause, 1 for the second clause). The last two elements define whether each temporal formula, ϕ_F or ϕ_G , is in CNF or DNF form (0 for CNF, 1 for DNF).

B. Evaluation of LTL-Explanations

We evaluate the utility of a candidate LTL-explanation by measuring the similarity between the target policy and a policy optimized for that LTL formula. A naive evaluation could simply generate a set of trajectories from the target policy and then count the trajectories that satisfy a formula. However, this approach would give high utility to “catch-all” LTL-explanations; that is, those containing disjunctions of all atomic predicates. We instead propose to measure utility as the weighted average of Kullback-Leibler (wKL) divergence values between the action distributions of the target policy and the policy optimized for a candidate LTL-explanation over randomly sampled states. More specifically, we first synthesize an FSPA-augmented MDP $\mathcal{M}_{\mathcal{A}}$ using a candidate LTL-explanation ϕ and use RL to optimize a policy with

respect to reward \tilde{r} (using Equation (1) or Equation (2)). We address the fact that multiple optimal policies can exist by optimizing N_{rep} replicates and choosing the policy with the highest policy entropy H^π , calculated as,

$$H^\pi = \frac{-\sum_{s \in \mathcal{B}_{\text{NT}}} A_\pi(s) \log A_\pi(s)}{|\mathcal{B}_{\text{NT}}|}, \quad (3)$$

where $A_\pi(s) := \pi(\cdot|s)$ is the action distribution for policy π at state s and \mathcal{B}_{NT} is a set of randomly sampled non-trap states (i.e., states $s \in \mathcal{S}$ whose corresponding automaton state is in $\mathcal{Q} \setminus \text{Tr}$).

We then measure the similarity between the selected policy and the target policy by calculating KL divergence values over action distributions of sampled states. More specifically, for a selected policy π_ϕ , target policy π_{tar} , and state s , we calculate,

$$D_{\text{KL}}(A_{\pi_\phi}(s) || A_{\pi_{\text{tar}}}(s)) = A_{\pi_\phi}(s) \log \frac{A_{\pi_\phi}(s)}{A_{\pi_{\text{tar}}}(s)}. \quad (4)$$

In cases where policies output multiple actions (as in our parking environment), the mean KL divergence value is used, averaged over the action distribution pairs. Finally, we use Equation (4) to calculate the utility U of LTL-explanation ϕ as a wKL divergence value over states $s_i \in \mathcal{B}_{\text{NT}}$,

$$U^\phi = - \sum_{i=1}^{|\mathcal{B}_{\text{NT}}|} w_i D_{\text{KL}}(A_{\pi_\phi}(s_i) || A_{\pi_{\text{tar}}}(s_i)), \quad (5)$$

where w_i is the weight associated with s_i . We calculate these weights as,

$$w_i = \frac{\bar{H}^{\pi_{\text{tar}}}(s_i)}{\sum_{s_j \in \mathcal{B}_{\text{NT}}} \bar{H}^{\pi_{\text{tar}}}(s_j)}, \quad (6)$$

where $\bar{H}^{\pi_{\text{tar}}}(s)$ is a normalized entropy calculated as,

$$\bar{H}^{\pi_{\text{tar}}}(s) = 1 + \frac{A_{\pi_{\text{tar}}}(s) \log A_{\pi_{\text{tar}}}(s)}{H_{\text{max}}}, \quad (7)$$

and H_{max} is the maximum possible entropy. We use a weighted average to emphasize similarity between policies at states where the target policy is highly certain about what action to take.

We include an augmented return filter to ignore any LTL-explanations that produce a policy with a converged return lower than a user-defined threshold \tilde{R}_{th} . This filter thus ignores explanations that are impossible to satisfy given the FSPA-augmented MDP.

C. Neighborhood Definition and Evaluation

After evaluating an LTL-explanation ϕ , our search proceeds by generating a neighborhood $\mathcal{N}(\phi)$ of related explanations. We define the neighborhood $\mathcal{N}(\phi)$ as the set of explanations whose row vector representations differ from that of ϕ at a single location (i.e., a single bit-flip). We note that the class of LTL formulae considered in this paper (i.e., of the form $\mathcal{F}(\phi_F) \wedge \mathcal{G}(\phi_G)$) are completely connected under this notion of a neighborhood. After generating $\mathcal{N}(\phi)$, we evaluate each of the neighboring explanations using the method discussed in Section III-B.

Algorithm 1: TL Greedy Local-Search

Input: number of searches N_{search} , number of maximum search steps N_{max} , number of replicates N_{rep} , number of sampled episodes N_{ep} , reward filter threshold \tilde{R}_{th}

Output: LTL-explanation ϕ

```

1: Construct empty buffer  $\Phi$ 
2: for  $n = 1, 2, \dots, N_{\text{search}}$  do
3:   Initialize starting explanation  $\phi$  randomly
4:   for  $m = 1, 2, \dots, N_{\text{max}}$  do
5:      $B = \text{EvalNeighbors}(\phi, N_{\text{rep}}, N_{\text{ep}}, \tilde{R}_{\text{th}})$ 
6:      $\phi_{\text{max}}, U_{\text{max}} = B[0]$ 
7:     if  $\phi = \phi_{\text{max}}$  then
8:       for  $i = 1, 2, \dots, N_{\text{extend}}$  do
9:          $\phi', U' \leftarrow B[i]$ 
10:         $B' = \text{EvalNeighbors}(\phi', N_{\text{rep}}, N_{\text{ep}}, \tilde{R}_{\text{th}})$ 
11:         $\phi'_{\text{max}}, U'_{\text{max}} \leftarrow B'[0]$ 
12:        if  $U'_{\text{max}} > U_{\text{max}}$  then
13:           $\phi, U \leftarrow \phi'_{\text{max}}, U'_{\text{max}}$ 
14:          break
15:        if  $\phi = \phi_{\text{max}}$  then break
16:        else  $\phi, U \leftarrow \phi_{\text{max}}, U_{\text{max}}$ 
17:      Store  $(\phi, U)$  to  $\Phi$ 
18: return  $\phi$  from  $\Phi$  with the highest  $U$ 

```

D. Additional Neighborhood Expansion & Extension

To address the potential existence of multiple undesired local optima, we also include additional neighborhood expansion and extension steps in our search. The expansion step creates an expanded neighborhood $\mathcal{N}_{\text{exp}}(\phi)$ for a given parent explanation ϕ by flipping the values of the last two elements (i.e., the elements that define whether the temporal formulae are in CNF or DNF) of each explanation in the original neighborhood $\mathcal{N}(\phi)$. These additional explanations are then evaluated. This expansion step is implemented if the original neighborhood of ϕ does not produce a better explanation than ϕ .

We also include an extension step that forces the search to generate and evaluate neighborhoods for the child explanations in $\mathcal{N}(\phi)$, even when the explanations in $\mathcal{N}(\phi)$ have a lower utility than ϕ . That is, we extend the search by evaluating neighbors of the explanations in $\mathcal{N}(\phi)$ with the highest utilities, up to N_{extend} times. This extension step is implemented if the original and extended neighborhoods of ϕ do not produce a better explanation than ϕ .

IV. RESULTS

A. Test Environments and RL Training Details

We demonstrated our proposed method in two environments: a game of capture-the-flag (CtF) and a car-parking scenario. The CtF game is a discrete grid-world environment with two agents and complex adversarial dynamics. If the two agents are next to each other in the blue territory, then the red agent is killed with 75% probability (and vice versa in

Algorithm 2: EvalNeighbors()

Input: starting explanation ϕ_{in} , number of replicates N_{rep} , number of sampled episodes N_{ep} , reward filter threshold \tilde{R}_{th}

Output: Sorted buffer $B = [(\phi_i, U^{\phi_i})]$

```

1: Generate  $\mathcal{N}(\phi_{\text{in}})$  and construct sorted buffer  $B$ 
2: for  $\phi_i$  in  $\mathcal{N}(\phi_{\text{in}})$  do
3:   Synthesize automaton from  $\phi_i$ 
4:   Optimize and evaluate  $N_{\text{rep}}$  policies for  $\phi_i$ 
5:   Choose the policy with highest  $U^{\phi_i}$ 
6:   Calculate average return  $\bar{R}$  for  $N_{\text{ep}}$  episodes
7:   if  $\bar{R} > \tilde{R}_{\text{th}}$  do store  $(\phi_i, U^{\phi_i})$  to  $B$ 
8:    $\phi_{\text{max}}, U_{\text{max}} = B[0]$ 
9:   if  $\phi_{\text{max}} = \phi_{\text{in}}$  then repeat Lines 2-7 for  $\mathcal{N}_{\text{exp}}(\phi_{\text{in}})$ 
10: return  $B$ 

```

the red territory). The game ends when either agent captures its opponent's flag or the blue agent is killed. The state space is fully observable, and there are 5 discrete actions for an agent: stay, up, right, down, and left. We aimed to explain the policy used by the blue agent and defined the red agent to use a heuristic policy focused on defending its territory border (highlighted in Figure 2a). We defined four atomic predicates based on distances between objects in the environment: $\psi_{\text{RA,BF}} = d_{\text{RA,BF}} < 1.0$, $\psi_{\text{BA,RF}} = d_{\text{BA,RF}} < 1.0$, $\psi_{\text{BA,RA}} = d_{\text{BA,RA}} < 1.5$, $\psi_{\text{BA,BT}} = d_{\text{BA,BT}} < 1.0$, where BA, BF, BT, RA, and RF stand for the blue agent, blue flag, blue territory, red agent, and red flag, respectively, and $d_{\text{Obj}_1, \text{Obj}_2}$ is the euclidean distance between objects Obj_1 and Obj_2 . The resulting search space contained 640 explanations. We used the reward function defined in Equation (1).

We used the car-parking scenario to test our method's ability to scale to continuous state spaces, as shown in Figure 2b. We used the parking environment from [20], modified to include another vehicle that the ego vehicle must avoid when trying to reach the landmark parking spot. An episode terminates when the ego vehicle reaches the landmark, hits a wall, or hits the other vehicle. The state space is continuous and fully observable, and there are two continuous actions: steering angle and acceleration. We aimed to explain the policy used by the ego vehicle and defined the other vehicle to use a heuristic policy that moves left or right based on a random initial location. We defined three distance-based atomic predicates for this environment: $\psi_{\text{ego,goal}} = d_{\text{ego,goal}} < 1$, $\psi_{\text{ego,other}} = d_{\text{ego,other}} < 3$, $\psi_{\text{ego,wall}} = d_{\text{ego,wall}} < 4$, where ego and other stand for the ego and other vehicles, respectively. The resulting search space contains 96 explanations. We used the reward function defined in Equation (2).

We used proximal policy optimization (PPO) [21] to optimize our target and candidate explanation policies for the CtF game, and soft actor critic (SAC) [22] with hindsight experience replay (HER) [23] for the parking environment. We used the following search hyperparameters: $N_{\text{max}} = 10$, $N_{\text{extend}} = 3$, $N_{\text{st}} = 5,000$, $N_{\text{ep}} = 200$, and $\tilde{R}_{\text{th}} = 0.05$.

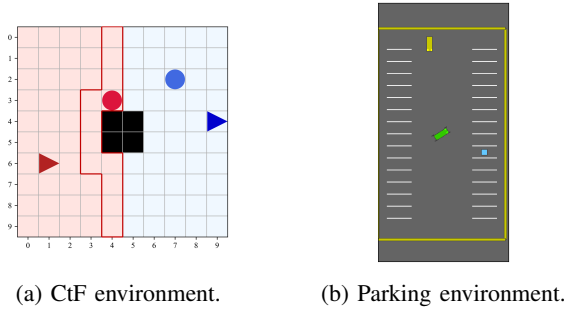


Fig. 2: a) CtF game. Black squares are obstacles, triangles are flags, and circles are agents. The region highlighted by solid red lines is the border region for the red agent. b) Parking environment. The green rectangle is the ego vehicle, the blue square is the landmark, and the yellow rectangle is the other vehicle. Yellow walls mark the boundary.

B. CtF Experiment Results

We defined the target policy for the blue agent as an RL policy optimized for $\mathcal{F}(\psi_{BA,RF} \wedge \neg\psi_{RA,BF}) \wedge \mathcal{G}(\neg\psi_{BA,RA} \vee \psi_{BA,BT})$, which requires that: “Eventually, the blue agent reaches the red flag and the red agent does not reach the blue flag. Globally, the blue agent does not encounter the red agent or it stays in the blue territory.” We optimized three replicates for this explanation and chose the one with the highest entropy, calculated using Equation (3).

Table I shows the explanations found by our search algorithm over 10 random starts. We see that Searches 1 and 5 successfully found the true target explanation as the explanation with the highest utility among searched explanations. Search 1 searched 8.13% of the search space while Search 5 searched 10.2% of it. The second best search result is Search 6, whose explanation is: “Eventually, the blue agent captures the red flag. Globally, the blue agent is not inside the blue territory while the red agent does not capture the blue flag, or the blue agent does not encounter the red agent.” This explanation is close to the target explanation and consistent with the game dynamics. For example, the task (i.e., $\mathcal{F}(\phi_F)$) part of the explanation includes the overall objective of the blue agent capturing the red flag, while the constraint (i.e., $\mathcal{G}(\phi_G)$) part plausibly captures the battle dynamics of our environment which could incentivize the blue agent to avoid the red agent if it is outside of the blue territory, but engage the red agent if both agents are in the blue territory. Figure 3 shows a partial trace of the search tree produced by Search 5. We see that the extension step discussed in Section III-D was used in the third step of the search, which successfully kept the search from getting stuck in a sub-optimal local minimum early in the search process. Though not shown here, the extension step was also used in the terminating neighborhood before finding the optimal solution.

C. Parking Experiment Results

We defined the target policy of the ego vehicle as an RL policy optimized for $\mathcal{F}(\psi_{ego,goal}) \wedge \mathcal{G}(\neg\psi_{ego,other} \wedge$

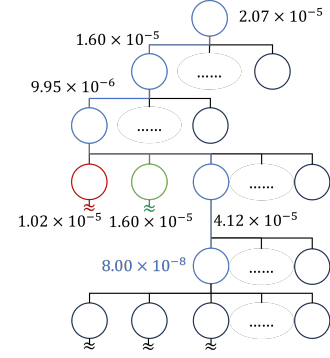


Fig. 3: A partial trace of Search 5 from Table I. Circles represent nodes with their corresponding wKL divergence values shown. The blue nodes and lines show how the local minimum moved as the search proceeded.

$\neg\psi_{ego,wall}$), which requires that: “Eventually, the ego vehicle reaches the goal. Globally, the ego vehicle does not hit the other vehicle and walls.” We again optimized two replicates and chose the one with the highest entropy.

Table II shows the explanations found by our search algorithm over 8 random starts. Searches 1, 5, and 7 successfully found the true target explanation, with each searching 37.5%, 29.2%, and 33.3% of the search space, respectively. The second best results were Searches 6 and 8, which found the same solution whose explanation is: “Eventually, the ego vehicle encounters the other agent. Globally, the ego vehicle does not reach the goal or does not hit the wall.” This explanation captures a failure case, where the ego vehicle sometimes does not reach the goal because it collides with the other vehicle, though it does successfully avoid walls. This result suggests that the resulting explanation from a search can capture unlikely, but observed, behaviors from the target policy that occur due to the stochastic nature of the environment.

V. CONCLUSIONS

This paper introduces a method for generating an explanation of a given RL policy using a connected class of LTL formulae. We achieve this through a local-search algorithm with multiple starting points applied to the class of LTL formulae, resulting in an associated policy that minimizes the weighted KL divergence from the target policy. To validate our approach, we generated target policies using user-defined LTL formulae for two simulations and show that our proposed method successfully identifies each target explanation. Future directions include automated methods for determining an appropriate set of atomic predicates and implementing transfer learning techniques to efficiently optimize policies for candidate explanations.

REFERENCES

- [1] D. Silver, T. Hubert, J. Schrittwieser, *et al.*, “A general reinforcement learning algorithm that masters chess, shogi, and go through self-play,” *Science*, vol. 362, no. 6419, pp. 1140–1144, 7, 2018.

TABLE I: CtF experiment search results. The target policy was successfully found in Searches 1 and 5.

Search	LTL-explanation	wKL div. [-]	Searched specs [%]
1	$\mathcal{F}(\psi_{BA,RF} \wedge \neg\psi_{RA,BF}) \wedge \mathcal{G}(\neg\psi_{BA,RA} \vee \psi_{BA,BT})$	8.00×10^{-8}	8.13
2	$\mathcal{F}((\neg\psi_{RA,BF}) \vee (\psi_{BA,RF})) \wedge \mathcal{G}(\neg\psi_{BA,RA} \vee \psi_{BA,BT})$	5.95×10^{-6}	9.06
3	$\mathcal{F}((\neg\psi_{BA,RA}) \vee (\neg\psi_{RA,BF})) \wedge \mathcal{G}((\psi_{BA,BT}) \vee (\psi_{BA,RF}))$	8.52×10^{-5}	6.56
4	$\mathcal{F}(\neg\psi_{BA,BT} \wedge \neg\psi_{RA,BF}) \wedge \mathcal{G}((\neg\psi_{BA,RF}) \vee (\neg\psi_{BA,RA}))$	1.57×10^{-6}	6.56
5	$\mathcal{F}(\psi_{BA,RF} \wedge \neg\psi_{RA,BF}) \wedge \mathcal{G}(\neg\psi_{BA,RA} \vee \psi_{BA,BT})$	8.00×10^{-8}	10.2
6	$\mathcal{F}(\psi_{BA,RF}) \wedge \mathcal{G}((\neg\psi_{BA,BT} \wedge \neg\psi_{RA,BF}) \vee (\neg\psi_{BA,RA}))$	7.42×10^{-7}	8.44
7	$\mathcal{F}(\psi_{BA,RA}) \wedge \mathcal{G}((\neg\psi_{BA,BT}) \vee (\neg\psi_{BA,RF} \wedge \neg\psi_{RA,BF}))$	1.18×10^{-5}	8.59
8	$\mathcal{F}(\neg\psi_{BA,BT}) \wedge \mathcal{G}((\neg\psi_{BA,RA} \wedge \psi_{BA,RF}) \vee (\neg\psi_{RA,BF}))$	1.46×10^{-7}	6.56
9	$\mathcal{F}((\psi_{BA,RA}) \wedge (\neg\psi_{BA,RF})) \wedge \mathcal{G}((\psi_{BA,BT}) \vee (\neg\psi_{RA,BF}))$	1.18×10^{-5}	11.4
10	$\mathcal{F}((\psi_{RA,BF}) \vee (\neg\psi_{BA,BT})) \wedge \mathcal{G}((\neg\psi_{BA,RA}) \vee (\psi_{BA,RF}))$	1.62×10^{-5}	7.19

TABLE II: Parking experiment search results. The target policy was successfully found in Searches 1, 5, and 7.

Search	LTL-explanation	wKL div. [-]	Searched specs [%]
1	$\mathcal{F}(\psi_{ego,goal}) \wedge \mathcal{G}(\neg\psi_{ego,other} \wedge \neg\psi_{ego,wall})$	0.00	37.5
2	$\mathcal{F}(\neg\psi_{ego,other} \wedge \psi_{ego,wall}) \wedge \mathcal{G}(\neg\psi_{ego,goal})$	7.35×10^{-4}	28.1
3	$\mathcal{F}(\neg\psi_{ego,other} \wedge \psi_{ego,wall}) \wedge \mathcal{G}(\neg\psi_{ego,goal})$	7.35×10^{-4}	27.1
4	$\mathcal{F}(\psi_{ego,wall}) \wedge \mathcal{G}(\neg\psi_{ego,goal} \vee \psi_{ego,other})$	6.40×10^{-4}	30.2
5	$\mathcal{F}(\psi_{ego,goal}) \wedge \mathcal{G}(\neg\psi_{ego,other} \wedge \neg\psi_{ego,wall})$	0.00	29.2
6	$\mathcal{F}(\psi_{ego,other}) \wedge \mathcal{G}(\neg\psi_{ego,goal} \vee \neg\psi_{ego,wall})$	4.61×10^{-4}	44.8
7	$\mathcal{F}(\psi_{ego,goal}) \wedge \mathcal{G}(\neg\psi_{ego,other} \wedge \neg\psi_{ego,wall})$	0.00	37.5
8	$\mathcal{F}(\psi_{ego,other}) \wedge \mathcal{G}(\neg\psi_{ego,goal} \vee \neg\psi_{ego,wall})$	4.61×10^{-4}	33.3

- [2] S. Zhang, L. Yao, A. Sun, and Y. Tay, “Deep learning based recommender system: A survey and new perspectives,” *ACM Comput. Surv.*, vol. 52, no. 1, 5:1–5:38, 2019.
- [3] H. Ju, R. Juan, R. Gomez, K. Nakamura, and G. Li, “Transferring policy of deep reinforcement learning from simulation to reality for robotics,” *Nat. Mach. Intell.*, vol. 4, no. 12, pp. 1077–1087, 2022.
- [4] J. Chen, S. E. Li, and M. Tomizuka, “Interpretable end-to-end urban autonomous driving with latent deep reinforcement learning,” *IEEE Trans. on Intell. Transp. Syst.*, vol. 23, no. 6, pp. 5068–5078, 2022.
- [5] A. Heuillet, F. Couthouis, and N. Díaz-Rodríguez, “Explainability in deep reinforcement learning,” *Knowledge-Based Syst.*, vol. 214, p. 106685, 28, 2021.
- [6] E. Bartocci, C. Mateis, E. Nesterini, and D. Nickovic, “Survey on mining signal temporal logic specifications,” *Inf. and Computation*, vol. 289, p. 104957, 1, 2022.
- [7] J.-R. Gaglione, D. Neider, R. Roy, U. Topcu, and Z. Xu, “Learning linear temporal properties from noisy data: A MaxSAT-based approach,” in *Automated Technology for Verification and Analysis*, Z. Hou and V. Ganesh, Eds., Cham: Springer Int. Publishing, 2021, pp. 74–90.
- [8] Z. Kong, A. Jones, and C. Belta, “Temporal logics for learning and detection of anomalous behavior,” *IEEE Trans. Automat. Control*, vol. 62, no. 3, pp. 1210–1222, 2017.
- [9] G. Bombara and C. Belta, “Offline and online learning of signal temporal logic formulae using decision trees,” *ACM Trans. Cyber-Phys. Syst.*, vol. 5, no. 3, 22:1–22:23, 2021.
- [10] R. Karagulle, N. Aréchiga, A. Best, J. DeCastro, and N. Ozay, “A safe preference learning approach for personalization with applications to autonomous vehicles,” *IEEE Robot. Automat. Lett.*, vol. 9, no. 5, pp. 4226–4233, 2024.
- [11] R. Yan, A. Julius, M. Chang, A. Fokoue, T. Ma, and R. Uceda-Sosa, “STONE: Signal temporal logic neural network for time series classification,” in *2021 Int. Conf. Data Mining Workshops (ICDMW)*, 2021, pp. 778–787.
- [12] D. Li, M. Cai, C.-I. Vasile, and R. Tron, “Learning signal temporal logic through neural network for interpretable classification,” in *2023 Amer. Control Conf. (ACC)*, 2023, pp. 1907–1914.
- [13] S. Jha, A. Tiwari, S. A. Seshia, T. Sahai, and N. Shankar, “TeLEx: Passive STL learning using only positive examples,” in *Runtime Verification*, S. Lahiri and G. Reger, Eds., Cham: Springer Int. Publishing, 2017, pp. 208–224.
- [14] S. Jha, A. Tiwari, S. A. Seshia, T. Sahai, and N. Shankar, “TeLEx: Learning signal temporal logic from positive examples using tightness metric,” *Formal Methods Syst. Des.*, vol. 54, no. 3, pp. 364–387, 1, 2019.
- [15] X. Li, Z. Serlin, G. Yang, and C. Belta, “A formal methods approach to interpretable reinforcement learning for robotic planning,” *Science Robot.*, vol. 4, no. 37, eaay6276, 18, 2019.
- [16] R. S. Sutton, D. Precup, and S. Singh, “Between MDPs and semi-MDPs: A framework for temporal abstraction in reinforcement learning,” *Artificial Intell.*, vol. 112, no. 1, pp. 181–211, 1, 1999.
- [17] M. L. Littman, “Markov games as a framework for multi-agent reinforcement learning,” in *Mach. Learn. Proc. 1994*, W. W. Cohen and H. Hirsh, Eds., San Francisco (CA): Morgan Kaufmann, 1, 1994, pp. 157–163.
- [18] K. Schneider, “Improving automata generation for linear temporal logic by considering the automaton hierarchy,” in *Proc. Artificial Intell. Logic Program.*, ser. LPAR ’01, Berlin, Heidelberg: Springer-Verlag, 2001, pp. 39–54.
- [19] A. Duret-Lutz, E. Renault, M. Colange, *et al.*, “From spot 2.0 to spot 2.10: What’s new?” In *Computer Aided Verification*, S. Shoham and Y. Vizel, Eds., Cham: Springer Int. Publishing, 2022, pp. 174–187.
- [20] E. Leurent, *An environment for autonomous driving decision-making*, <https://github.com/eleurent/highway-env>, 2018.
- [21] J. Schulman, F. Wolski, P. Dhariwal, A. Radford, and O. Klimov, *Proximal policy optimization algorithms*, 28, 2017. arXiv: [1707.06347](https://arxiv.org/abs/1707.06347) [cs].
- [22] T. Haarnoja, A. Zhou, P. Abbeel, and S. Levine, “Soft actor-critic: Off-policy maximum entropy deep reinforcement learning with a stochastic actor,” in *Proc. of the 35th Int. Conf. Mach. Learn.*, PMLR, 3, 2018, pp. 1861–1870.
- [23] M. Andrychowicz, F. Wolski, A. Ray, *et al.*, “Hindsight experience replay,” in *Advances in Neural Inf. Process. Syst.*, vol. 30, Curran Associates, Inc., 2017.